On the Influence of Reynolds Number on the Mach Stem Height at Shock Reflection from a Circular Cylinder

E.V. Timofeev, A. Hakkaki-Fard, H. Kleine, and B.W. Skews

1 Introduction

The transition from so-called regular to irregular shock wave reflection has been the subject of considerable research effort over the last seven decades [1]. The most thoroughly investigated case is that of the straight wedge. Viscosity can significantly influence the transition process [2, 3], and a relative increase of the role viscous forces play in the flow (equivalent to a lowering of the Reynolds number) typically results in a delay of the establishment and development of an irregular reflection pattern [4]. In the straight wedge case, the influence of viscosity is more pronounced close to the transition (detachment) point [4]. The case of a cylindrical obstacle has been investigated in a number of studies, and experimental results indicate that the regular reflection pattern, identified by visual inspection of experimental images, appears to be maintained longer on the cylindrical surface when compared to the straight wedge case [5]. This finding is, however, at variance with recent numerical results [6, 7, 8]. They show that in the inviscid case the transition occurs at the same wall angle as for the straight wedge. This implies that only the local wall angle determines whether or not transition will occur while the preceding history of the reflection off the first portion of the cylinder has no influence on the actual transition point. However, if one includes viscous effects in the simulation, CFD predicts a delay of the transition [7, 8], which is qualitatively similar to the observations made for the straight wedge case.

Previous experimental results indicate an influence of cylinder radius on the reflection transition: the perceived persistence of regular reflection appears to be more pronounced the smaller the cylinder radius is, and the transition angle is seen to approach the straight wedge value for large cylinder radii [5]. The experimental measurements [5] and numerical predictions for the same Reynolds number range

E.V. Timofeev · A. Hakkaki-Fard
McGill University, Dept. of Mechanical Engineering, Montreal, QC, H3A0C3, Canada

H. Kleine
University of New South Wales, School of Engineering and Information Technology, Canberra, ACT 2600, Australia

B.W. Skews
University of the Witwatersrand, Flow Research Unit, Johannesburg 2050, South Africa

R. Bonazza and D. Ranjan (eds.), *29th International Symposium on Shock Waves 2*,
DOI: 10.1007/978-3-319-16838-8_86

[7, 8] differ, however, substantially in quantifying this delay – in the experiments, the delay amounts to several degrees while it is only a fraction of a degree in the simulation. In the context of this study, the Reynolds number is defined as $\mathrm{Re} = \rho_1 V_S R/\mu_1$, where V_S is the speed of the shock, R is the cylinder radius, and ρ_1 and μ_1 are density and dynamic viscosity, respectively, of the gas in its initial state.

Previous experimental studies have attempted to determine the transition point from regular to irregular reflection by visual inspection of the obtained flow visualisation records. Numerical simulations indicate that in its early stages the Mach stem may only be a few micrometers long [6], which is undetectable with typical optical visualisation systems, even if high-resolution recording material is used. Higher image magnification improves the spatial resolution and allows one to resolve smaller features, but while this approach reduces the aforementioned discrepancy between predicted transition point and first detection of a Mach stem, imaging limitations do not allow one to eliminate it [9]. Currently, neither single image nor time-resolved visualizations are capable to detect minuscule flow features with a characteristic length below ~ 0.05 mm, such as, in this case, the Mach stem. The experimental results reported in the literature [5] indicate that the aforementioned discrepancy for the transition angle decreases if the cylinder radius is increased – in view of the preceding discussion this can largely be attributed to a more favorable ratio of the size of the observed object and the spatial resolution of the recording medium.

Thus, at present it appears futile to attempt a direct detection of the actual transition point by means of optical flow visualisation. For this reason, it was decided in this work to observe the subsequent development of the irregular reflection and to deduce the influence of viscosity from fully established reflection patterns.

2 Experimental Details and Numerical Simulation

Time-resolved shadowgraph visualisation with a high-speed video camera (Shimadzu HPV-1) is the key diagnostic tool for the experiments. The camera is typically run at its maximum frame rate of 10^6 frames per second (fps) with an exposure time of 250 ns. The spatial resolution of the camera is 312×260 pixels.

All tests are conducted with air as test gas in a standard shock tube with rectangular cross section (150 mm high, 75 mm wide) and a test section with a 215 mm diameter field of view. The shock Mach number M_S is determined from time-of-arrival data obtained by means of three KISTLER pressure transducers mounted flush with the shock tube wall ahead of and within the test section. The nominal values for the shock Mach number in these tests are $M_S = 1.22$ and $M_S = 1.34$. With a given set of different diaphragms, these shock Mach numbers can be obtained for different initial pressures p_1 in the test section. In the described experiments, p_1 ranges from 6.3 kPa to the ambient value of 95 kPa. The tests are conducted at ambient temperature, which is in the range $293\,K \leq T_1 \leq 298\,K$. Two models of different diameter are mounted on the floor and on the ceiling of the test section. The models are half-cylinders made of aluminium and have a polished surface finish with a roughness better than $0.5\,\mu$m. The model radius R is accurate within ± 0.025 mm and is varied by a factor of 4 – the used radii are 75 mm and 18.75 mm, respectively.

The measurements of the polar angle θ_P from individual image analysis that takes into account image distortions and possible position errors of the degree scale, are accurate within $\pm 0.1^\circ$. With the aforementioned ranges of p_1 and R, the Reynolds number Re (defined in the previous section) can vary between approximately 32,000 and 2×10^6. In the tests by Takayama & Sasaki [5], p_1 was kept constant in the shock Mach number range investigated here, and Re varied as a function of cylinder radius between approximately 500,000 and 8.8×10^6.

Using two models in the same experiment has the advantage that such tests are fully free from any problems related to shot-to-shot repeatability of the shock tube as both models are subjected to the same shock wave. However, in visualizations that show both models, one pixel corresponds to a physical size of 0.35 mm, and hence objects smaller than this value cannot be resolved. The image magnification in the available optical system can be more than doubled so that the detectable size threshold is lowered to about 0.155 mm, but in this case, the field of view is reduced so that only one of the models can be seen.

Numerical simulations were carried out using the Navier-Stokes equations with the Sutherland viscosity law and calorically perfect gas assumption ($\gamma = 1.4$) for air. The non-slip boundary condition with a specified temperature (equal to T_1) was used on the cylinder wall. The inviscid result was obtained using the Euler equations and the impermeable wall boundary condition. Details on the numerical method and code are given by [10] and [7]. The background unstructured grid consisting of triangular elements was subjected to local adaptive transient refinement/coarsening in the vicinity of localized flow features (shock fronts, contact surfaces, boundary layers etc.). For viscous computations, grid refinement was performed in such a way so that to approximate with sufficient accuracy the distribution of gasdynamic variables across shock fronts for all Reynolds numbers. Grid convergence studies were conducted, and the results in Fig. 2 may be considered as grid-independent.

3 Results

The height h of the Mach stem, the associated polar angle θ_P of the incident shock location, and the equivalent wall angle θ_W are defined as shown in Fig. 1a. In the tests described here, the initial polar angle for both models is 0° and measurements are taken up to a maximum polar angle of $(\theta_P)_{\max} \approx 90^\circ$. Tests in which both models are imaged confirm that within the aforementioned measurement accuracy, the dimensionless Mach stem height h/R is constant for the same polar angle θ_P – hence the Mach stem height scales with cylinder size, as predicted for an inviscid flow. The associated Reynolds numbers for each cylinder differ by a factor of four (approx. 500,000 vs. 2×10^6), which is seen to have no measurable effect. A typical visualisation record for the two-model configuration is given in Fig. 1b.

The aforementioned increase of the image magnification and the resulting reduction in field of view mean that multiple tests have to be run for different models. In order to clarify how much the measured non-dimensional Mach stem height h/R would change as a function of inevitable variations in M_S (in the investigated range, the shock Mach number can be reproduced within ± 0.012, with a measurement

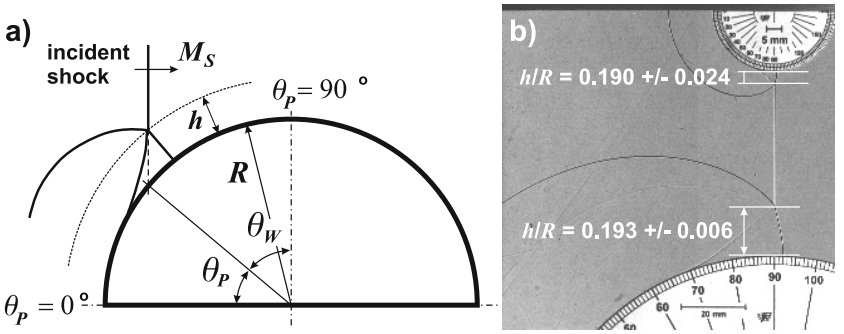

Fig. 1 (**a**) Definition of the Mach stem height h and the associated polar and wall angles θ_P and θ_W for a developed Mach reflection on a cylindrical surface; (**b**) Visualisation of reflection patterns at $\theta_P = 90^\circ$ for two models with radii 18.75 mm and 75 mm, $M_S = 1.23$

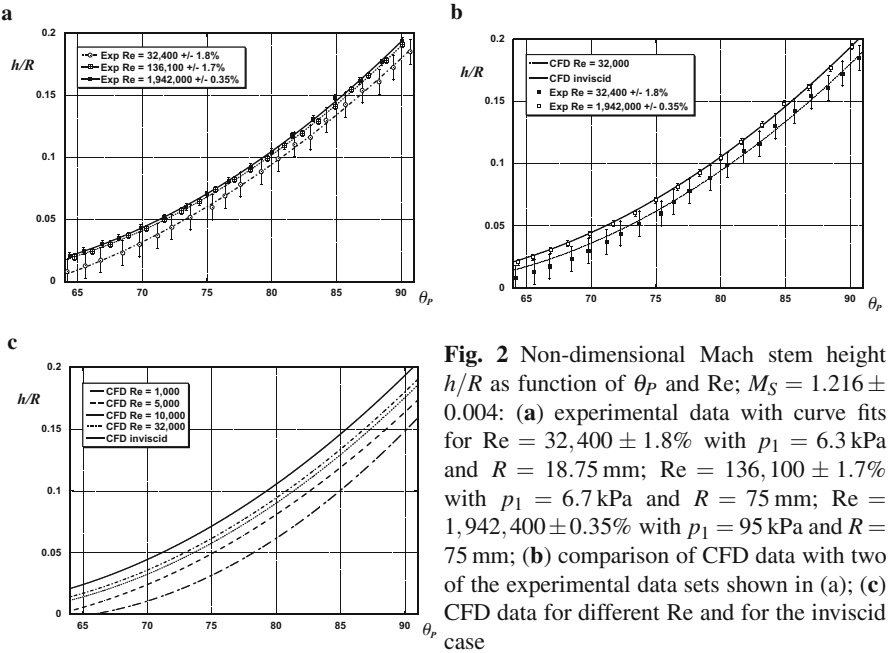

Fig. 2 Non-dimensional Mach stem height h/R as function of θ_P and Re; $M_S = 1.216 \pm 0.004$: (**a**) experimental data with curve fits for $\mathrm{Re} = 32,400 \pm 1.8\%$ with $p_1 = 6.3$ kPa and $R = 18.75$ mm; $\mathrm{Re} = 136,100 \pm 1.7\%$ with $p_1 = 6.7$ kPa and $R = 75$ mm; $\mathrm{Re} = 1,942,400 \pm 0.35\%$ with $p_1 = 95$ kPa and $R = 75$ mm; (**b**) comparison of CFD data with two of the experimental data sets shown in (a); (**c**) CFD data for different Re and for the inviscid case

uncertainty of ± 0.002 in each test), tests were conducted in which the shock Mach number was deliberately varied by larger amounts than the usual spread. As one would expect, h/R increases with increasing M_S but the difference is of the same order as the measurement uncertainty for h/R (± 0.0025) for a Mach number deviation of approximately half the typical experimental spread. On the basis of these results and equivalent numerical simulations it may be concluded that only tests with shock Mach numbers deviating not more than ± 0.006 from the nominal value can be considered as being equal as far as the obtained reflection patterns are concerned. Equivalently, for tests with such nominally equal Mach numbers but different

Reynolds numbers only variations of h/R larger than the measurement uncertainty will be considered as measurable deviations.

The development of the (dimensionless) Mach stem height h/R with polar angle θ_P is shown in Fig. 2a for three tests conducted at $M_S = 1.216 \pm 0.004$. While the shock Mach numbers were identical in all tests (within measurement accuracy), the Reynolds numbers differed by a factor of approximately 15 and 60, respectively. Lowering only the initial pressure p_1 has only a minute influence on the Mach stem development, and only a combined reduction of p_1 and R yields a clearly identifiable difference. This indicates a strongly nonlinear influence of the Reynolds number. As the optical system is unchanged in both tests, the uncertainty in geometrical measurements is increased by the same factor by which the cylinder radius is decreased. In spite of a partial and slight overlapping of the error bar ranges of the curves, the measurements indicate a clear trend, namely that the Mach stem height at a given polar angle is consistently decreasing with decreasing Reynolds number and that the angle at which it becomes visible increases if Re is decreased. On the smaller cylinder (18.75 mm radius), the Mach stem becomes indiscernible for polar angles below 65°. At this angle, the Mach stem is already clearly visible on the larger model (75 mm radius) – even in the case of a low p_1. The shown experimental data indicate that a Reynolds number reduction by at least two orders of magnitude to levels of $\mathrm{Re} \approx 10^4$ is required to detect a discernible change in Mach stem height. Such Reynolds numbers are at the lower limit of the performance range of normal shock tubes.

The measured data are in excellent qualitative and quantitative agreement with numerically predicted ones, as shown in Fig. 2b. In shock tubes of conventional size, such as the one used here, Reynolds numbers lower than 10^4 are difficult to achieve, and hence the experimentally detectable differences in the reflection pattern are of the order of magnitude shown in Fig. 2a,b. Numerical simulations for Reynolds numbers further lowered down to 10^3 clearly show the aforementioned nonlinear relationship between Re and the Mach stem development (Fig. 2c): the influence of Re is small in typical Reynolds number regimes for shock tubes ($\mathrm{Re} \geq 10^5$) but it increases substantially if the Reynolds number is further lowered, most notably for $\mathrm{Re} \leq 10^4$. An experimental confirmation of this behaviour is, however, hard to obtain because of the aforementioned difficulties to establish such low Reynolds numbers in shock tubes of conventional size.

Both experimental and numerical data also show that the growth rate of the Mach stem exhibits, in the presented range of polar angles, a near-identical behaviour for all investigated Reynolds numbers above 10^4 – the primary difference between the curves is the offset. This suggests that the main influence of a decreasing Reynolds number is to impede the initial establishment of the Mach stem, but that the influence is diminished once the Mach stem has erupted.

4 Conclusions

• The Reynolds number, which in typical shock tube applications is $\sim 10^5 \div 10^6$, influences the establishment of the reflection pattern, but this influence appears to be minute unless Re is changed by more than two orders of magnitude to $\lesssim 10^4$;

• It appears unlikely that measurable differences in the reflection pattern can be achieved by changing only the size of the cylinder, at least in shock tubes of conventional size. It is therefore likely that the transition delays reported in the literature as a function of cylinder radius R are mostly caused by insufficient optical resolution.
• In the observed range of polar angles, the differences in the fully developed reflection patterns remain constant for all studied Reynolds numbers, which indicates similar growth rates but considerably different offsets. This would mean that the Reynolds number primarily influences the initial establishment of the Mach stem and only to a lesser extent its subsequent growth;
• A sufficiently large change in the Reynolds number can therefore be seen to influence the reflection pattern in a qualitatively similar fashion to what has been observed for straight wedges, namely that a lowering of the Reynolds number results in a persistence of regular reflection beyond the theoretical transition angle;
• In the straight wedge case, the regular reflection pattern persists because the boundary layer behind the reflection point effectively modifies the wall angle, keeping it above the detachment angle [2, 3, 4]. The further away the wedge angle is from the transition (detachment) angle the greater modification is required, which is equivalent to requiring thicker boundary layers (lower Re). In the case of a reflection off a cylinder, the wedge angle changes continuously, so that the values which are close to the detachment angle are only attained over a short duration and distance during the reflection process. This could explain why in this case a substantial change in Reynolds number is required to observe a clearly measurable influence.

Acknowledgements. The study is supported by NSERC Discovery grant 298232-2009. E.T. acknowledges the support by SEIT, UNSW Canberra, during his sabbatical leave in 2011-2012.

References

1. Ben-Dor, G.: Shock Wave Reflection Phenomena, 2nd edn. Springer (2007)
2. Hornung, H.G., Oertel, H., Sandeman, R.J.: JFM 90, 541–560 (1979)
3. Hornung, H.G., Taylor, J.R.: JFM, 123, 143-153 (1982)
4. Henderson, L.F., Takayama, K., Crutchfield, W.Y., Itabashi, S.: JFM 431, 273-296 (2001)
5. Takayama, K., Sasaki, M.: Rep. Inst. High Speed Mech., Tohoku Univ., Japan, 46, 1-30 (1983)
6. Timofeev, E., Skews, B.W., Voinovich, P., Takayama, K.: Proc. 22nd Int. Symp. on Shock Waves, 2, pp. 1231–1236. Univ. of Southhampton (1999) ed. by G.J. Ball, R. Hillier, G.T. Roberts
7. Hakkaki-Fard, A.: PhD thesis, McGill University, Montreal, QC (2011), `http://digitool.Library.McGill.CA:80/R/-?func=dbin-jump-full&object_id=106502 &silo_library=GEN01`
8. Hakkaki-Fard, A., Timofeev, E.: Determination of the sonic point in unsteady shock reflections using various techniques based on numerical flowfield analysis. In: Kontis, K. (ed.) Proc. 28th Int. Symp. on Shock Waves, 2nd edn., pp. 643–648. Springer (2012)
9. Kleine, H., Tetreault-Friend, M., Timofeev, E., Gojani, A., Takayama, K.: On the Ongoing Quest to Pinpoint the Location of RR-MR Transition in Blast Wave Reflections. In: Hannemann, K., Seiler, F. (eds.) Proc. 26th Int. Symp. on Shock Waves, 2nd edn., pp. 1455–1460. Springer (2007)
10. Drikakis, D., Ofengeim, D., Timofeev, E., Voinovich, P.: Computation of non-stationary shock-wave/cylinder interaction using adaptive-grid methods, J. J. Fluids & Struct. 11, 665–691 (1997)